RE: SOURCE

Final report for the project

Innovative Manufacturing Processes for CIGS Targets for Solar Cell Applications

Project period: July 2017 until December 2017
Project number: 44271-1

Med stöd från:
VINNOVA
Energimyndigheten
FORMAS
STRATEGISKA INNOVATIONS-PROGRAM

SLUTRAPPORT
1

Date
2018-03-15

Dnr
2017-001990

Projektnr
44271-1

Titel på projektet – svenska Innovativa tillverkningsprocesser för CIGS mål för solcellstillämpningar
Titel på projektet – engelska Innovative Manufacturing Processes for CIGS Targets for Solar Cell Applications
Universitet/högskola/företag Chalmers University of Technology
Adress Chalmers University of Technology Nuclear chemistry/Industrial Materials Recycling SE-412 96 Gothenburg Sweden
Namn på projektledare Marcus Hedberg
Namn på ev övriga projektdeltagare Midsummer AB
Nyckelord: 5-7 st CIGS, Sintering, SPS, High density,

Med stöd från:
VINNOVA
Energimyndigheten
FORMAS
STRATEGISKA INNOVATIONS-PROGRAM

Acknowledgements

This project was funded by the Swedish energy authority. All materials used in the project was supplied by Midsummer AB and all spark plasma sintering was performed at the Swedish SPS facility at Stockholm University. Special thanks are directed to Mirva Eriksson for help and guidance with the spark plasma sintering experiment.

Table of Contents

Med stöd från: VINNOVA Energimyndigheten FORMAS STRATEGISKA INNOVATIONS-PROGRAM

Sammanfattning

I det här projektet har ”spark plasma sintering” (SPS) studerats som en potentiell sintringsteknik för tillverkning av CIGS-målkroppar (sputtering targets). Både möjligheten till produktion av målkroppar från nya CIGS-pulver liksom tillverkning från återvunnet CIGS-pulver har undersökts. Möjlighet till återanvändning av gamla målkroppar genom återdeponering av pulver ovanpå tätsintrade målkroppar har också studerats. Resultaten visar att det går att tillverka tätsintrade målkroppar från både nya och återvunna CIGS- pulver med SPS teknik genom sintring vid 500-600 °C och sintringstider så korta som 3 minuter. De producerade målkropparna nådde densiteter av ungefär 95-97% av den teoretiska densiteten. Grovkrossade återvunna CIGS-pulver kunde sintras till täta kroppar utan behov av siktning av de krossade pulvren. Återdeponering av CIGS-pulver ovanpå redan sintrade kroppar kunde genomföras utan några problem med adhesion mellan pulvret och den redan sintrade substratytan.

Abstract

In this project the possibilities spark plasma sintering has been studied as a potential sintering technique for production of CIGS sputtering targets. Both the possibility for production of sputtering targets from virgin CIGS powders as well as powders recycled from used sputtering targets has been investigated. Potential reuse of old targets by re-deposition of CIGS powder onto already pressed and sintered compacts has also been studied. It was shown to be feasible to produce dense sintered compacts by spark plasma sintering from both new and recycled CIGS powders using sintering temperatures in the range of 500-600 °C and sintering times of 3 minutes. Densities achieved in the produced materials reach to about 95-97% of theoretical density. Coarse crushed recycled powders could be sintered into dense pellets without any need for particle sieving. Re-deposition of CIGS powder onto already sintered compacts could be performed without any adhesion problems between the powder and CIGS substrate.

Introduction

The production of Cupper-Indium-Gallium-Selenide (CIGS) based solar cells require deposition of the CIGS material onto the substrate surface that will constitute the final solar cell. Efficient material utilization can be reached by deposition of thin material films onto the solar cell surface. One technique for achieving production of thin films is by sputtering techniques where material is deposited onto a surface from a dense target [HSU 12]. When these sputtering targets have been used to the full extent of their individual usability during CIGS solar cell production they still contain CIGS material. This material is currently a waste fraction that potentially could be a source of material recycling within the production process. Recycling could be achieved either by collection, backing material removal from the sputtering target, crushing of the CIGS material and resintering into new sputtering targets or by deposition of additional CIGS material directly onto used sputtering targets. When sintering sputtering targets it is important to reach high density of the final sintered body in order to be able to produce a sputtering target suitable to deposit material from onto substrate surfaces. In CIGS sputtering targets production it has been reported that it is desirable to reach above 92% of the theoretical density in the sputtering target in order to have good performance during usage [HSU 15, NIN 10]. There are several techniques that can be applied in order to produce a dense compact from powder. When producing sputtering targets from CIGS powder hot pressing is a technique that previously has been applied [ZHO 14]. In hot pressing the material is pressed and sintered simultaneously by external heating of the pressing die during pressing. An alternative, similar technique, is spark plasma sintering (SPS). Spark plasma sintering is also a form of hot pressing technique but unlike conventional hot pressing, where the material is heated by an external source, the SPS process heats the sample directly by running current through the material and pressing die. This technique often allows for strongly reduced sintering times compared to sintering materials by hot pressing or conventional non-pressure assisted sintering. In this project SPS has been applied for the production of high density compacts of new as well as recycled CIGS material from used sputtering targets. The applicability of spark plasma sintering in production of CIGS sputtering targets has been investigated alongside with the possibility of re-depositing CIGS material onto a sputter target surface.

Experimental methods

The experimental work performed was divided between Chalmers University of Technology, where material preparation and pre- as well as post pressing analysis was performed. The spark plasma sintering experiments were performed at the National SPS facility in Stockholm. Both new CIGS powder and used sputtering targets were supplied by Midsummer AB.

Removal of Indium backing and sample crushing

The Indium metal backing material of the used CIGS sputtering targets was mechanically removed by grinding and polishing using Silicon carbide polishing paper. The used sputtering targets was then crushed in an agate mortar.

Spark Plasma Sintering Experiments

Sintering experiments was performed using an SPS-530 ET instrument placed in an Argon atmosphere glove box. Pressing dies with circular profile made of graphite was used during the sintering experiments. Also the pressing plungers used during sintering was made by graphite. During sample preparation the inside of the graphite pressing die walls was covered with an approximately 0.2 mm thick graphite paper. The graphite paper covering was done to prevent interaction between the pressing die and the sample itself in case of avoiding interactions causing the sample to sinter stuck to the die walls. The bottom plunger was inserted into the pressing die and also covered with graphite paper. Sample masses of about 2.5 g of new or recycled CIGS powder was added to the pressing die and the powder was covered with a graphite paper before inserting the top plunger. Graphite insulation was then put around the pressing die to reduce heat losses and homogenize temperature in the die during the sintering. The prepared sample was then pre-compacted before moving the sample into the glove box for sintering. The top and bottom electrode in the SPS-instrument was, just as the die and plungers, made of graphite and the temperature during sintering was controlled using a thermocouple inserted into a small drilled cavity in the outside of the pressing die. All sintering was performed under vacuum and the atmosphere was evacuated before the mechanical pressure was applied or the heating started. Sintering experiments was performed using pressures between 25-75 MPa. The pressure was set prior to heating was started and turned off when the set time for sintering had passed. A set sintering time at target temperature of 3 minutes was used for all sintering experiments. Sintering at temperatures of 400, 500, 550 and 600 °C was examined and the heating rate used was 100 °C/minute for all target temperatures except 550 °C where a heating ramp of 110 °C/minute was used instead. No controlled cooling was used during experiments and all samples where left to cool naturally by completely switching off the heating power after 3 minutes of sintering. Table 1 summarizes the SPS experiment performed and the parameters investigated.

Table 1. Sintering experiments performed using SPS. Sample 5 was made by depositing new recycled CIGS powder onto sample number 3. The top and bottom side of sample 3 was polished free from graphite before sintering of sample 5 was performed.

Sample number	CIGS material	Sintering Temp (°C)	Pressure (MPa)	Sintering Time (minutes)
1	New	400	50	3
2	Recycled	500	50	3
3	New	600	50	3
4	Recycled	600	50	3
5	Recycled on New	600	50	3
6	New	550	50	3
7	Recycled	550	50	3
8	New	500	50	3
9	Recycled	500	75	3
10	Mixed	550	50	3
11	Recycled	600	25	3

The graphite paper that got stuck to the sample pellets during sintering was removed by grinding using Silicon carbide polishing paper. Density determination of the produced pellets were performed by weighing and geometrical measurements of the produced pellets both prior to and after the pellets had been polished.

Results

Characterization of powders for Spark Plasma Sintering

Both the new CIGS as well as the recycled CIGS powders were characterized prior to spark plasma sintering experiments. The powders were characterized with respect to detectable crystalline phases as well as particle sizes of the new and recycled powders. X-ray powder diffraction (XRD) measurements of the powders confirmed that the powders mostly consisted of the CIGS materials. The new powder contained an additional crystalline phase that possibly could be attributed to indium selenide (InSe).

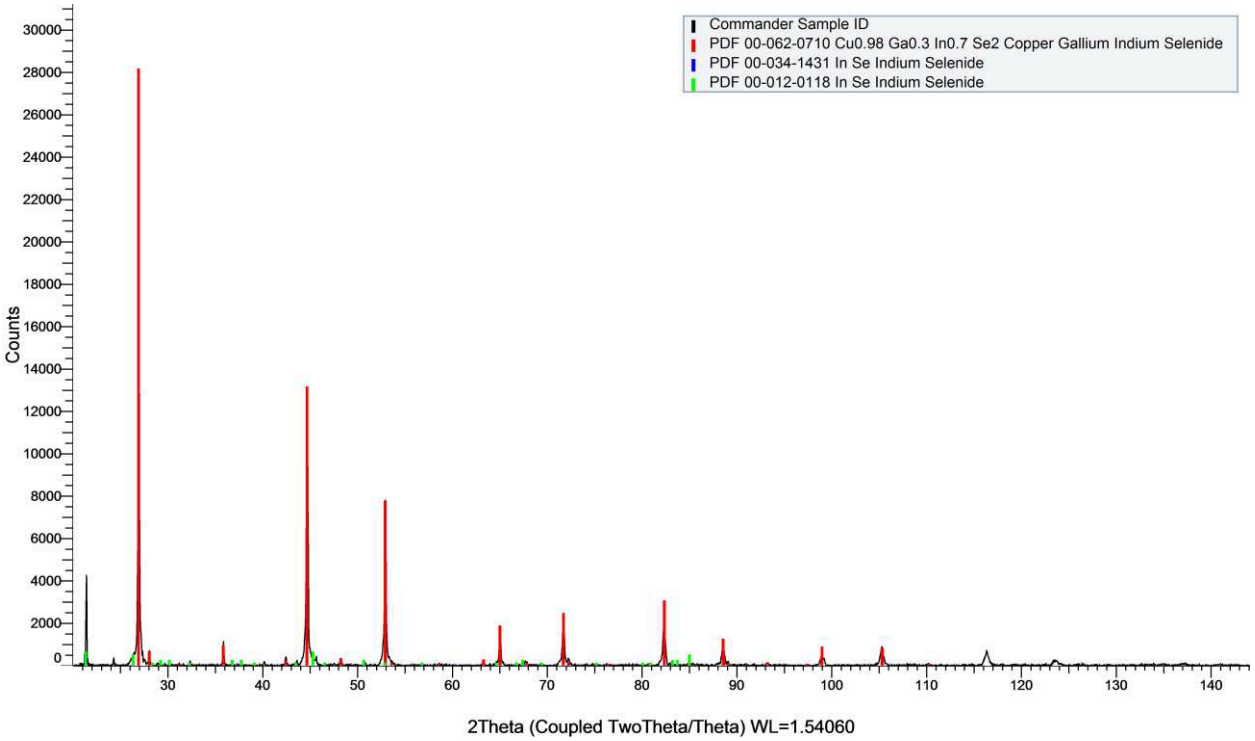

Figure 1. The X-ray diffractogram of the new CIGS powder.

In the material recycled from the CIGS sputtering targets there was no peaks observable part from the reflections coming from the CIGS material itself.

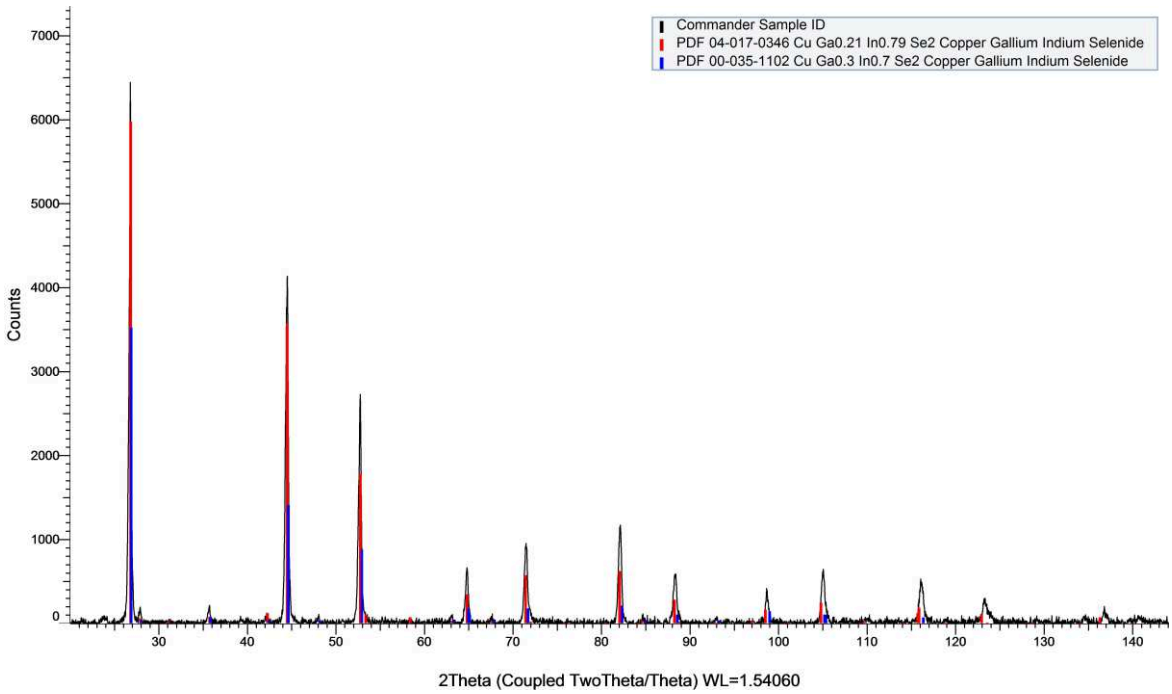

Figure 2. Diffractogram of the recycled CIGS material.

Usage of the CIGS sputtering targets seem to remove the InSe from the material, possibly by interdiffusion into the CIGS phase during sputtering process. In figure 2 it can also be observed that more than one CIGS phase can be reasonably well fitted to the diffractogram. This means that the substitution between In and Ga atoms in the crystal structure causes only minor shifts in the diffractogram and it becomes difficult for the XRD measurements to distinguish between any compositional changes in the two different CIGS materials. The CIGS peaks of the two diffractograms do however superpose each other very well indicating that there is no real reason to assume any large compositional changes in the used CIGS material compared to the new powder. Scanning electron microscopy was used to study the grain sizes in the new and recycled powders. The new CIGS powder is presented in figure 3.

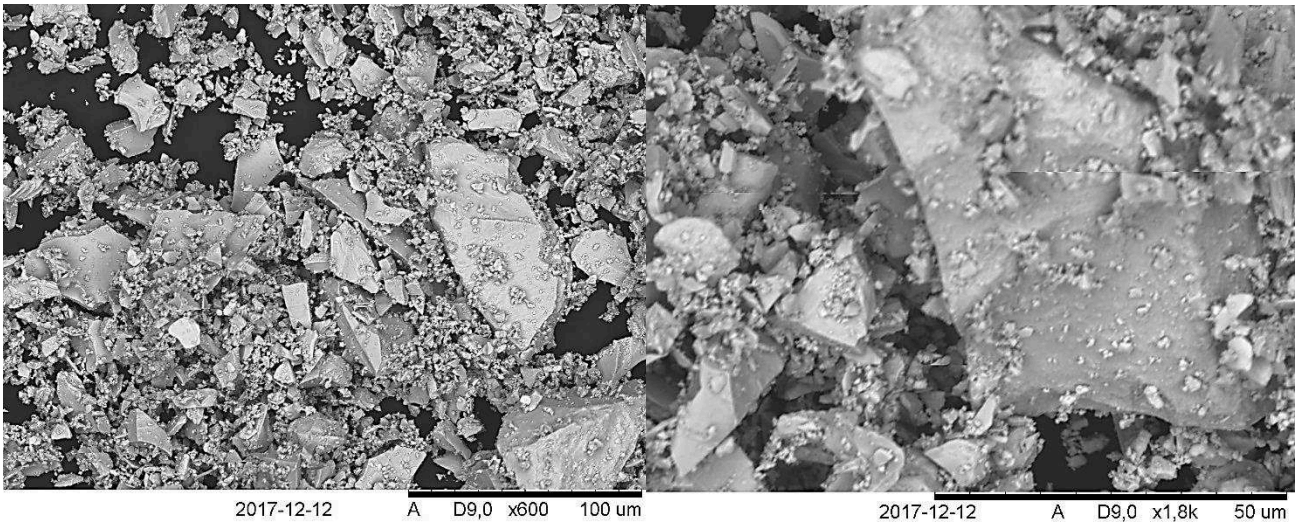

Figure 3. The new CIGS powder contained a span of size fractions, ranging from a small fraction of particles of around 100 µm length down to particles on the scale of a few micrometers.

The new powder did contain small amounts of particles with a characteristic length of about 100 µm but the major part of the powder was particles ranging from about 1 to 20 µm in size. The recycled sputtering targets were crushed using mortar and pestle and the resulting powder is presented in figure 4.

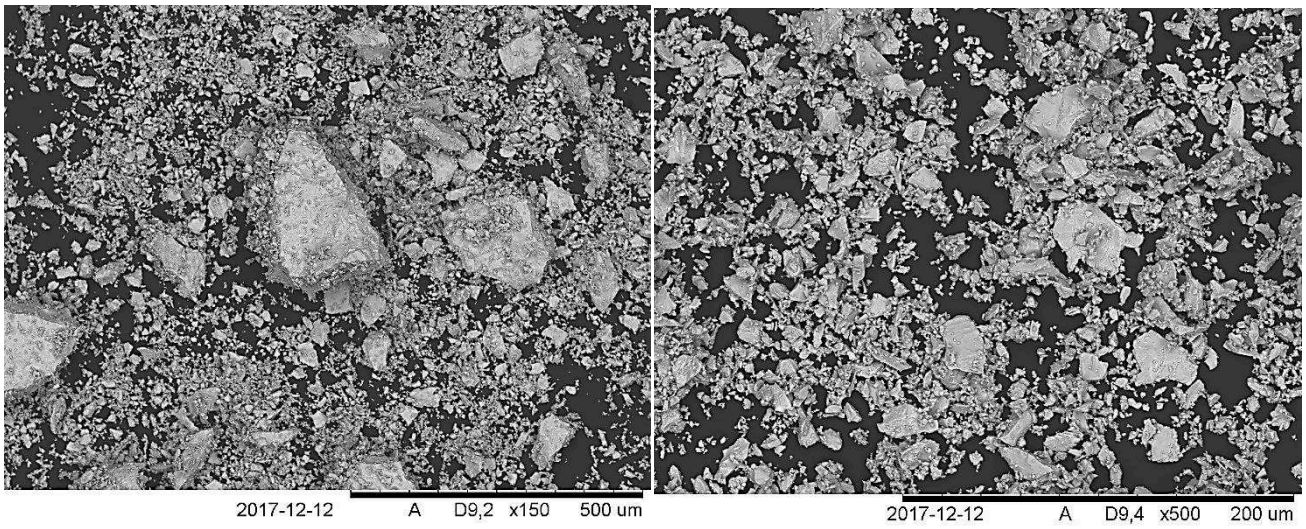

Figure 4. The resulting recycled powder after the CIGS targets had been crushed. The size fractions varied more within this powder with some particles in the 1 mm size range remaining.

The recycled powder became coarser than the new powder. There is still a fines fraction down on the scale of a few µm but on average the particles were larger and the recycled powder also contained some degree of big particles up to the size range of about 0.5-1 mm approximately.

Spark Plasma Sintering Results

In all of the sintering experiments performed it was possible to produce a final pellet. Table 2 lists the final densities achieved in the pellets produced. The standard deviations presented in table 2 are derived from uncertainty propagation of uncertainties in physical dimensions of the pressed sample pellets. The uncertainties in geometric pellet measurements were acquired by repeating the measurements of height and diameter 5 times for each pellet. The theoretical density used for calculation of %TD was 5.69 g/cm^3 [LI 15].

Table 2. Final dimensions, densities and percent of theoretical density achieved in the CIGS samples sintered.

Sample number	Mass (g)	Radius (cm)	Height (cm)	Density (g/cm3)	Standard deviation Density	% TD
1	2.564	0.505	0.771	4.15		72.95
2	2.241	0.508	0.504	5.49	0.033	96.44
3	2.200	0.520	0.515	5.13		90.10
4	2.222	0.512	0.496	5.45	0.096	95.85
5	2.880	0.506	0.681	5.27	0.064	92.56
6	2.136	0.510	0.475	5.49	0.162	96.54
7	2.260	0.507	0.510	5.48	0.090	96.33
8	2.273	0.502	0.522	5.50	0.047	96.63
9	2.203	0.507	0.500	5.45	0.085	95.72
10	2.076	0.504	0.469	5.55	0.097	97.60
11	2.426	0.518	0.550	5.24		92.12

The standard deviation of the measurements for samples 1, 3 and 11 are missing. In the case of sample 3 it is because it was reused as a mock up sputtering target for production of sample 5 and the sides of the samples were not polished graphite free enough to motivate replicate measurements of the physical dimensions of the sample. Sample 11 was not measured to establish measurement uncertainties because the top and bottom layer of graphite was not removed in order to be able to study the graphite deposit using scanning electron microscopy (SEM). Both sample 3 and 11 thus contain a slight bit of a bias since the residual graphite on those pellets contributes to lowering the average density of these samples. Sample 1 did not contain any residual graphite sheet on it after sintering at 400 °C. There was thus no problem with graphite influenced biases when measuring this sample but the low density and porous structure of the produced pellet resulted in damage of the sample when measuring. Therefore sample 1 was only measured once for height and diameter. The densities that could be reached generally varied in the area of 95-97% of theoretical density.

The sintering profile for all experiments performed are presented in figure 3. The figure presents the axial position change during the entire sintering experiment for each sample. The data is recorded and plotted so that shrinkage of the sintered samples is viewed as a positive change on the y-axis in the graph.

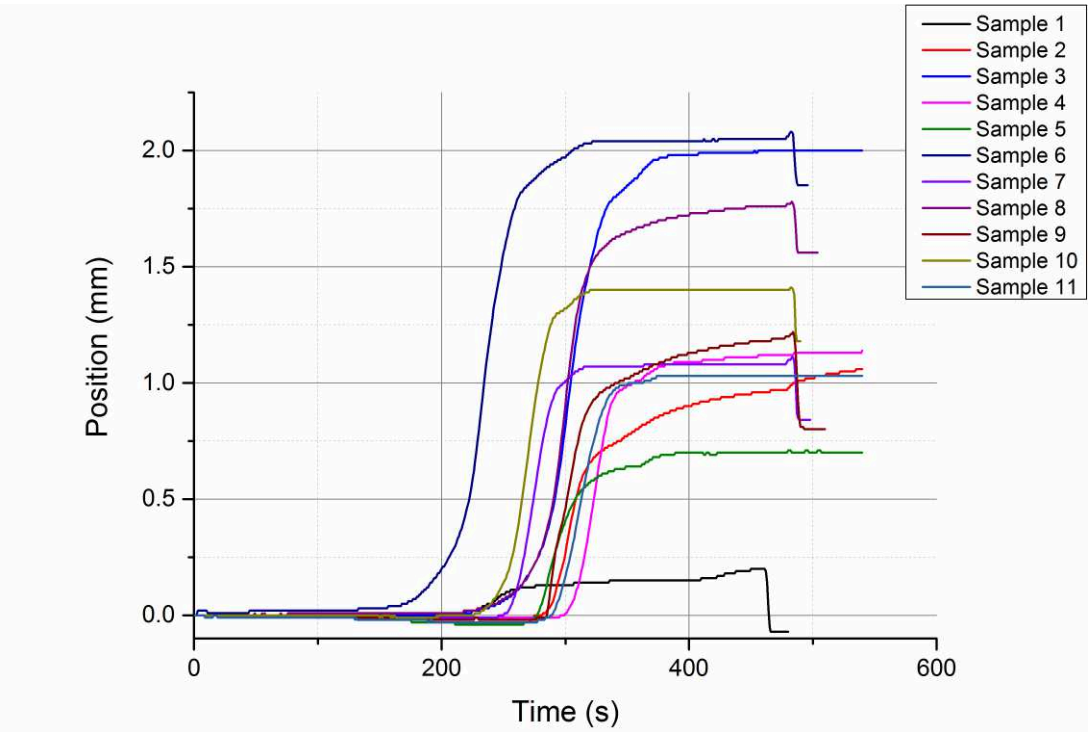

Figure 3. Positional axial change as a function of time of all sintered samples throughout their respective sintering experiments.

In the end of several of the sintering profile a sharp decrease can be observed. This sharp change does not correspond to any drastic change in the sample material but is an instrument effect and occurs when the compaction load is released after 3 minutes of sintering. Similarly a slight decrease in measured position can be observed in between about 150-250 seconds for many of the samples, this decrease is caused by thermal swelling of the materials and can be observed at temperatures before sintering phenomena starts to occur. By monitoring the starting point of sample compression it was possible to observe that the new and the recycled CIGS powders started to sinter at different temperatures. On average the new CIGS powder started to sinter at around 360 °C while recycled CIGS powder started to sinter at about 460 °C. The reason for this difference is not known but a possible reason is that the new and recycled powders contain somewhat different stoichiometry of Selenium compared to the recycled powders. This was more of a side note and not extensively investigated but it was observed that the pressure in the system increased at lower temperature and a bit more when sintering new CIGS powder compared to recycled powder.

The sintering kinetics was fast and when sintering at 550 or 600 °C the samples had more or less reached their final density already when the heating ramp was finished. At 550 and 600 °C some partial melting also occurred when sintering new CIGS powder and a small solidified droplet of CIGS could be observed at the edge between the pressing die and the top plunger after sintering. At 500 °C sintering a substantial part of the densification occurred during the 3 minutes of sintering time at target temperature. Figures 4 and 5 present examples of sintering and temperature profiles for sintering at 500 and 600 °C for new CIGS material.

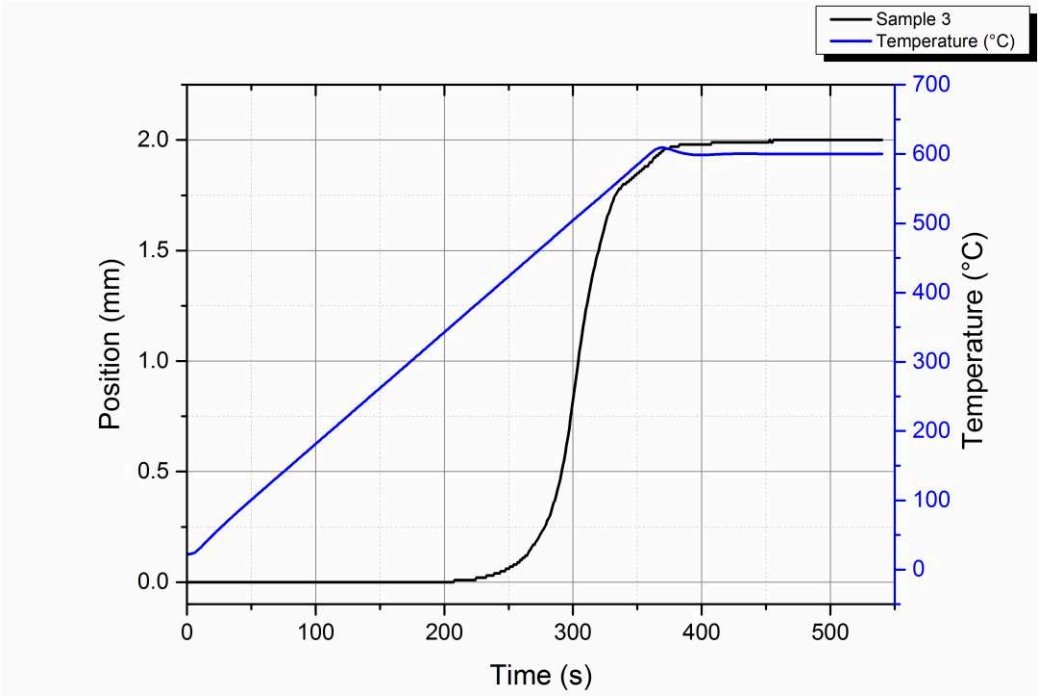

Figure 4. Sintering and temperature profile of sample 3 sintered at 600 °C.

In figure 4 it can be observed that when the sample reaches 600 °C the densification of the material is already close to almost completed and very little happens during the dwell time at 600 °C.

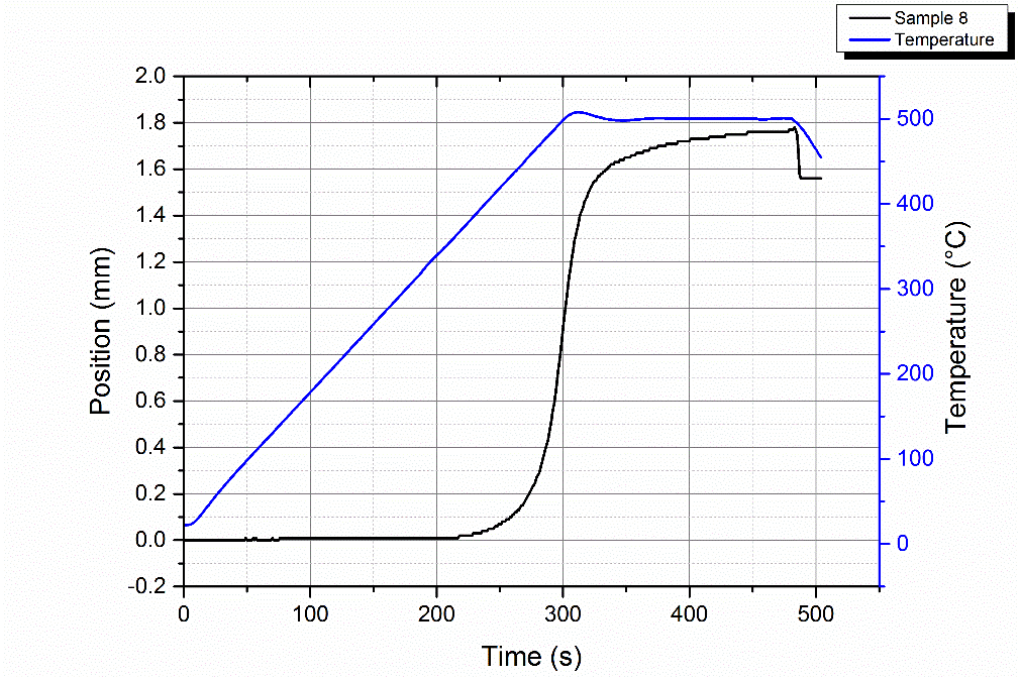

Figure 5. Sintering and temperature profile of sample 8 sintered at 500 °C.

When observing the sintering profile for sample 8 and compare it to sample 3 it would appear that the sintering is progressing slower compared to sintering at 600 °C since a significant part of the sintering is completed during the isothermal step of the sintering process. This is however a problematic comparison since the heating rate used is constant in both sintering experiments. This means that the sample sintered at 600 °C have sintered a minute longer than the 500 °C sample when both have reached their respective target sintering temperature. The densification profiles are also a bit difficult to compare since also small variations in amount of sample material and pre-compaction pressure influences the final material shrinkage during SPS. By plotting the sintering densification as percent of final pellet density as a function of sintering time it becomes more practical to make a general comparison between different samples.

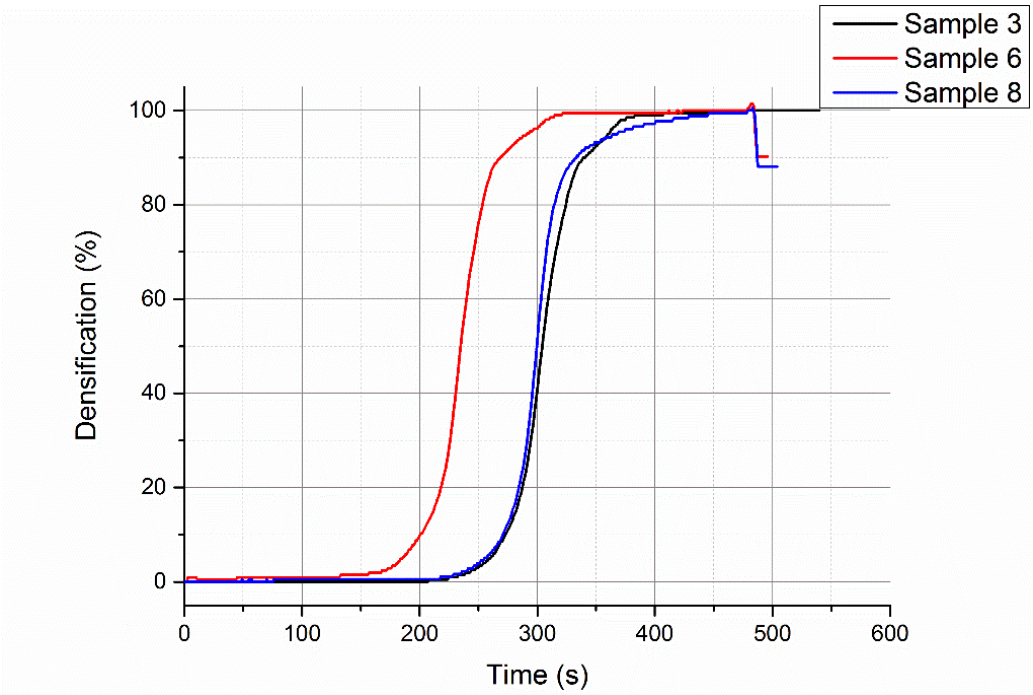

Figure 6. The sintering profiles of samples 3, 6 and 8 expressed as percent of final densification, where 0% indicates the non-sintered pellet and 100% is the final density reached in each individual pellet.

When comparing each sample to its individual final sintered density it becomes apparent that sintering progresses very similar during sintering at 500 and 600 °C respectively. In the end of the sintering profiles there seem to be a slightly lower densification rate for sample 8 compared to sample 3 but otherwise there is little difference in sintering at 500 or 600 °C. It does however appear that sintering progresses faster in sample 6, which is sintered at 550 °C. This is likely influenced of that a higher heating ramp (110 °C/min instead of 100 °C/min) is used during sintering at 550 °C, so sintering should occur earlier in sample 6 compared to the other samples when plotted against a time axis. This behavior is not only observed when sintering

the new CIGS material but a recurring trend in all the sintering experiments as is shown in figure 7.

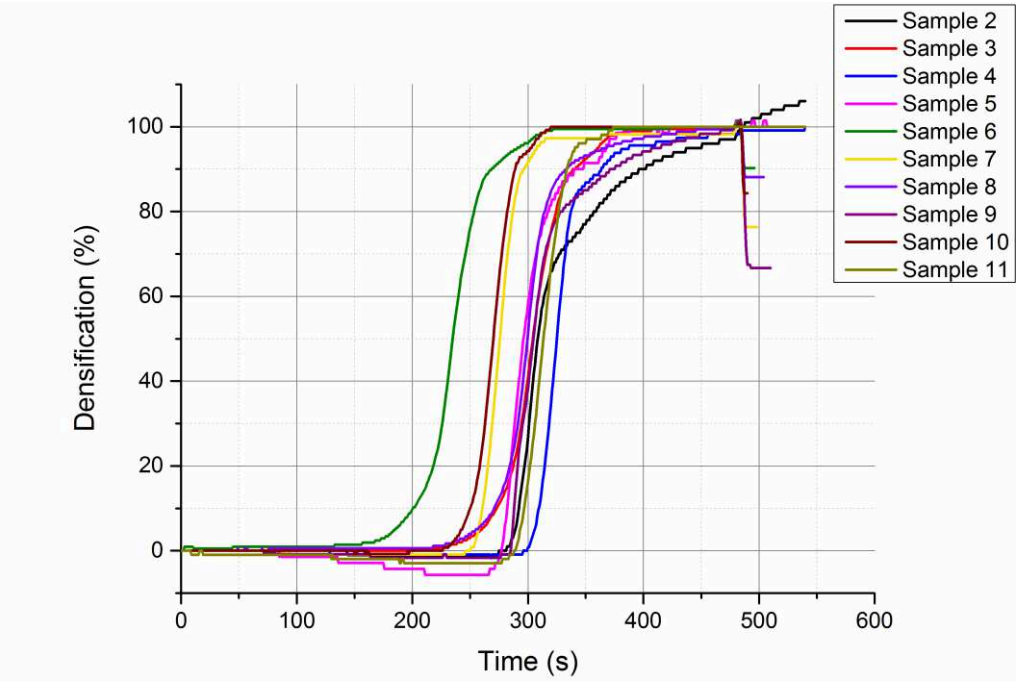

Figure 7. Sintering profiles for all the sintered samples, apart from sample 1, plotted as % of total densification as a function of time during the SPS process.

In figure 7 it can be observed that 3 sintering profiles, numbers 6, 7 and 10, start to sinter earlier compared to other samples. These are all the samples sintered at 550 °C where a higher heating rate was used while the other samples sinter fairly similarly with the exception that samples 3 and 8, which contain new CIGS, start to sinter a bit earlier than the samples containing recycled CIGS.

Sintered material characterizations

The sintered CIGS pellets were examined using SEM to compare the different microstructures of the produced pellets to each other and to the microstructure of the initial used sputtering targets that the CIGS material was recycled from.

Examination of the pellet sintered at 400 °C showed, similarly to the density measurements, that only very little sintering had occurred in the sample.

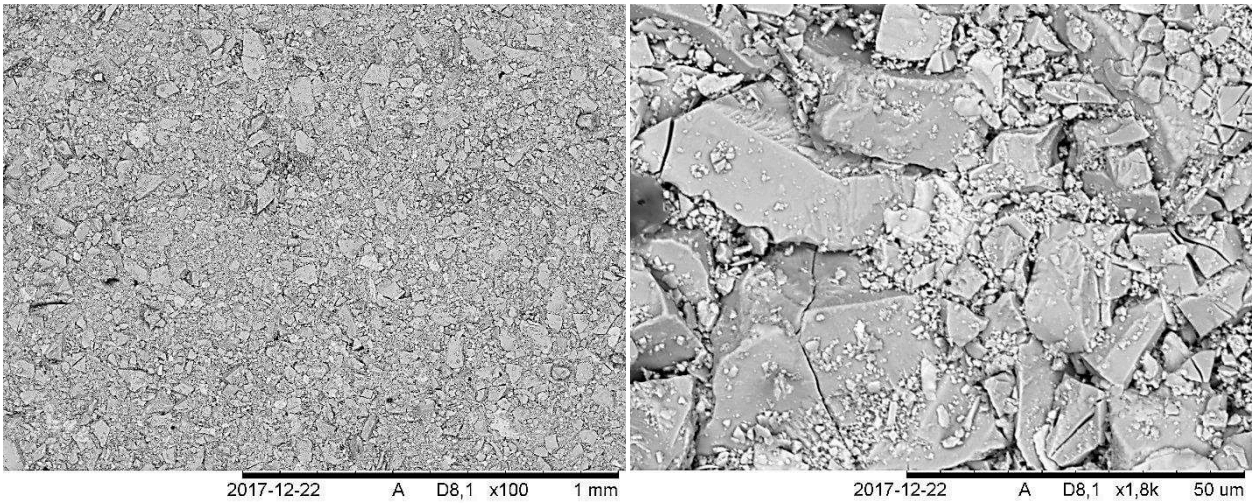

Figure 8. Microstructure of the topside of sample 1 sintered at 400 °C.

As can be observed in figure 8 no extensive grain boundary elimination occurred between the grains in the sample during sintering and the final more resembles a collection of individual particles than a single cohesive body.
Prior to crushing of the used sputtering targets were examined using SEM and the sputtering targets were densely sintered targets with grain sizes varying in the range of about 5-20 µm in general.

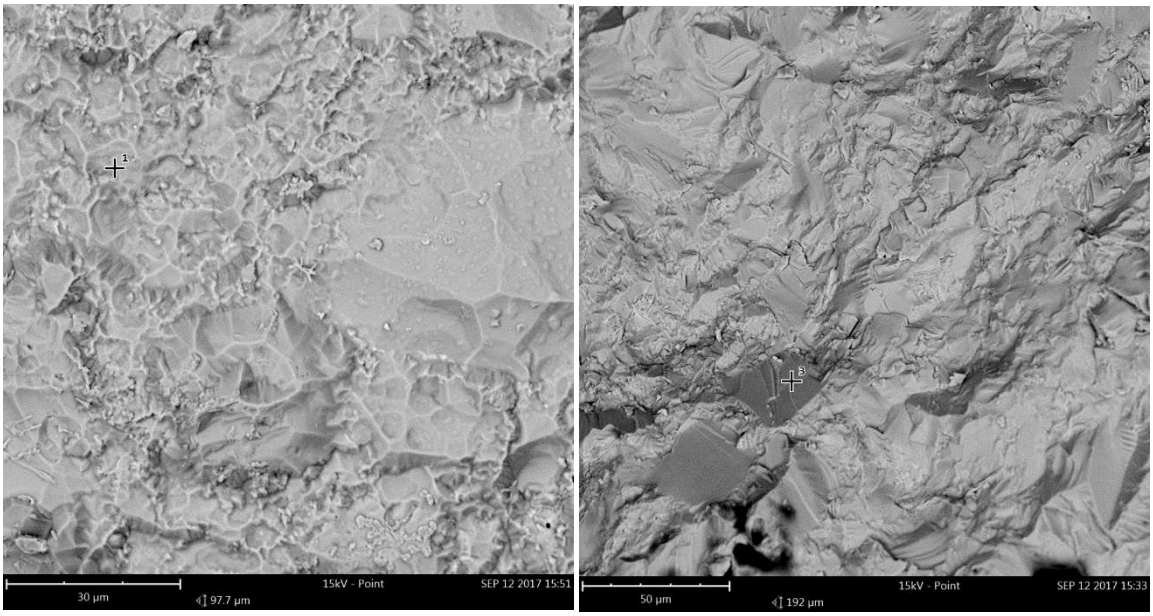

Figure 9. To the left: Grain structure of the used sputtering target. To the right: Cross section of the sputtering target.

It was very hard to identify any grain boundaries in any of the pellets sintered using SPS. Generally the samples looked like they partially had melted during sintering. This was true both for new and recycled CIGS powder.

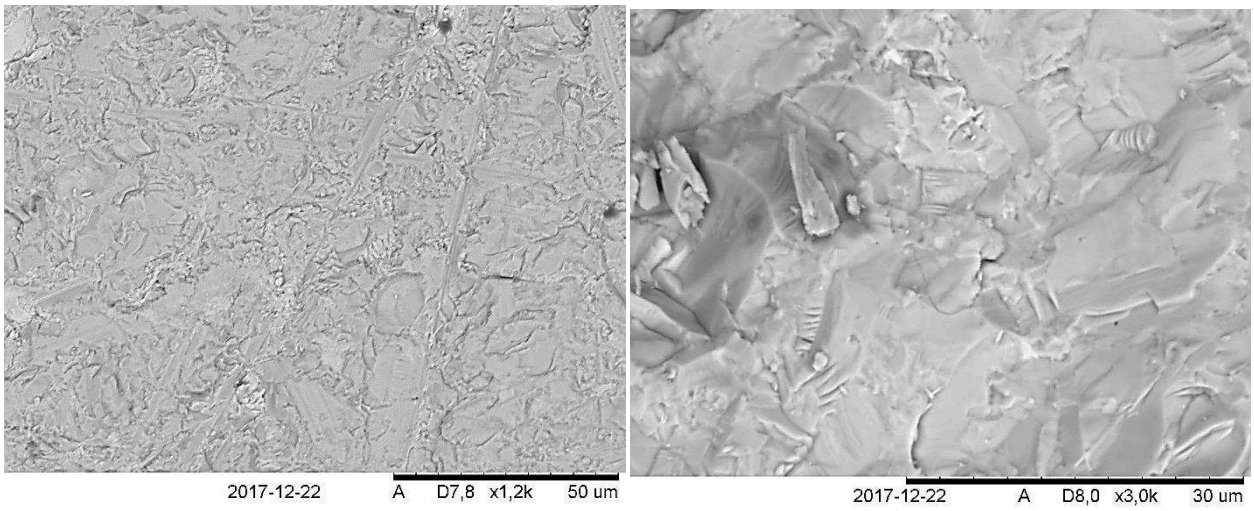

Figure 10. SEM images of pellets sintered using SPS. To the left: The surface of sample 8. To the right: The surface of sample 2. Both images were taken after the graphite had been removed from the surface of the sintered samples.

Samples 2 and 8 are used as examples of the microstructure of the sintered samples instead of showing the SEM images of each sample since all samples (apart from sample 1) displayed very similar microstructure. All samples looks like they may have partially melted during sintering or at least like a plastic flow mechanism has been contributing to the densification to a larger extent than grain boundary diffusion or lattice diffusion. This matter would however require further studies to determine definitely but it was observed that melting could occur at least when sintering new CIGS powder. The absence of formation of equally clearly defined grains as in figure 9 may also be influenced by the use of only 3 minutes sintering time which may be to short time for well-defined grains to form in the sintered samples in case of partial melting or plastic flow sintering mechanisms.
Investigation of the cross section of sample 5, the sample that contained recycled CIGS deposited onto sample 3, revealed that no boundary between the deposited material and substrate could be observed indicating that it should be feasible to deposit additional CIGS material onto used sputtering targets without having adhesion problems between the new and old layer.

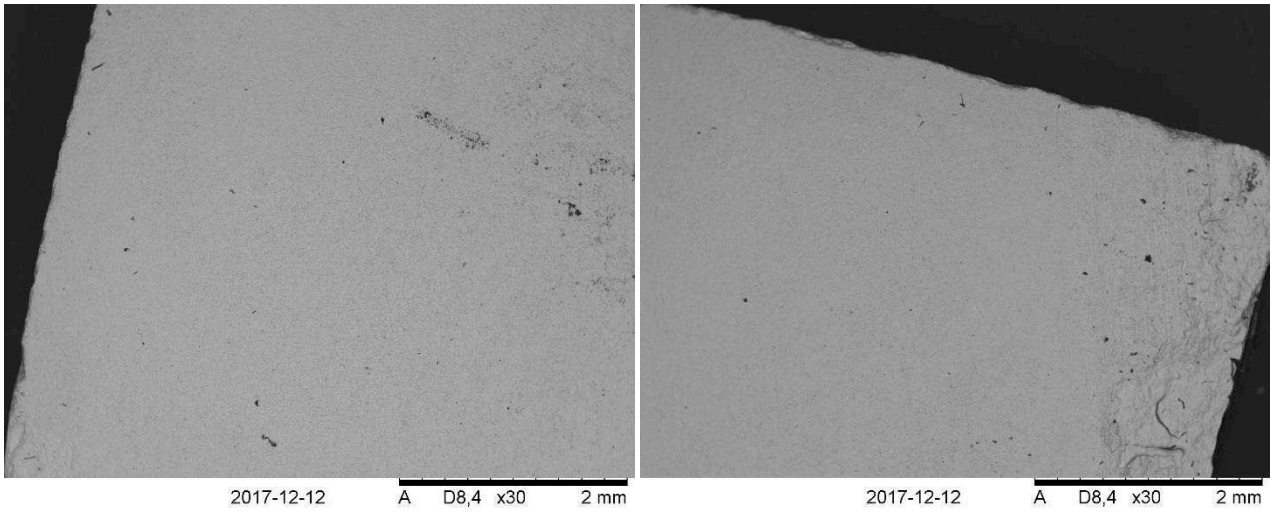

Figure 11. Cross section of sample 5. The pressed pellet was too thick to be captured in a single SEM image. The two images thus capture parts of the cross section and are together showing the entire thickness of the pellet. No layered separation between the substrate and the deposited material could be observed in the cross section of sample 5.

Additionally the graphite from the SPS process that deposited onto sample 5 was kept on one side to allow imaging of the interphase between the graphite sheet and the sample.

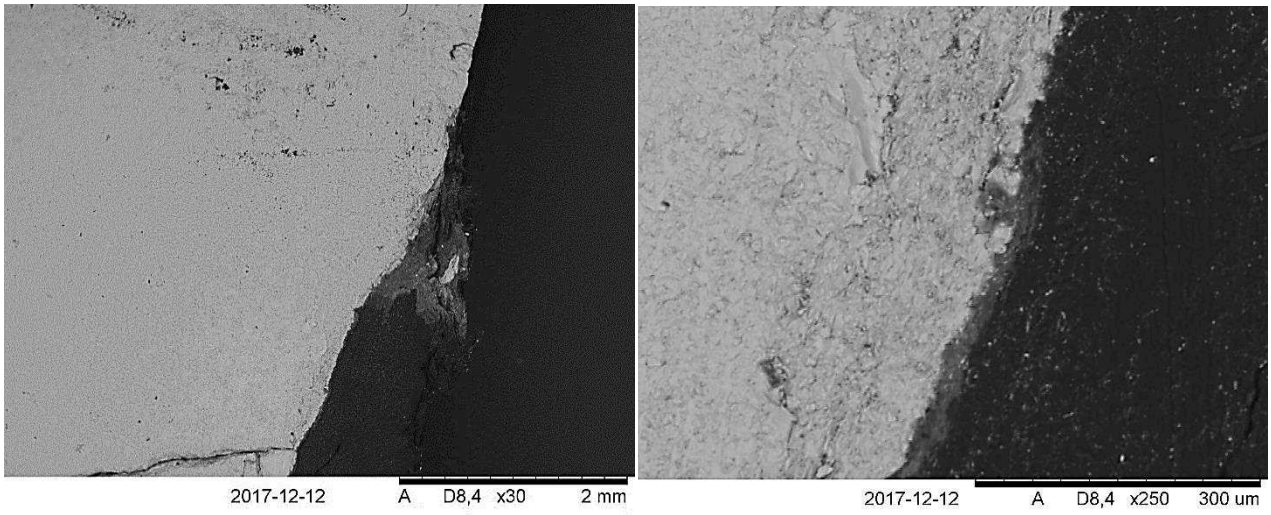

Figure 12. The graphite sheet adhesion layer to onto sample 5. The graphite sheet is sintered stuck to the CIGS material and needs polishing to be removed. No deep migration of graphite into the CIGS could be observed though.

The graphite could not be observed to deeply penetrate into the CIGS material which is expected due to the short sintering time used. Depending on the carbon sensitivity of the material in the sputtering process more sensitive surface element detection techniques may be required to determine a more exact carbon gradient into the CIGS

material but no real gradient of carbon into the sample could be detected by the energy dispersive X-ray spectroscopy (EDX) detector coupled to the electron microscope.

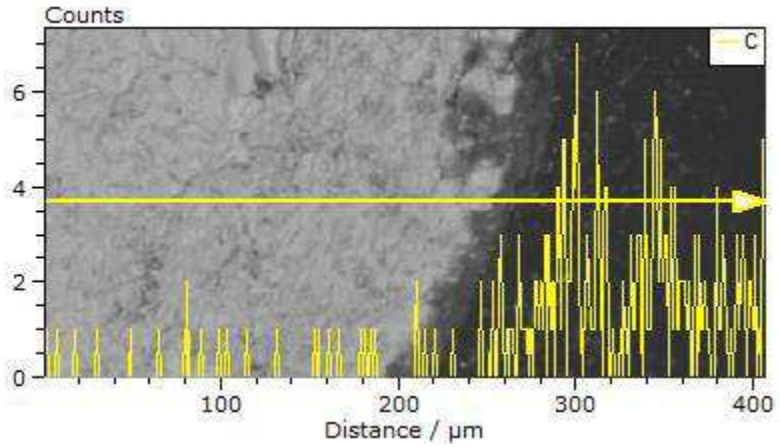

Figure 13. Line scan for carbon detection over the graphite/sample interphase using EDX. No clear diffusion gradient of carbon into the sample could be detected.

X-ray diffraction measurements was performed on sample 5 to confirm that no formation of undesired phases occurred in the sample material during sintering.

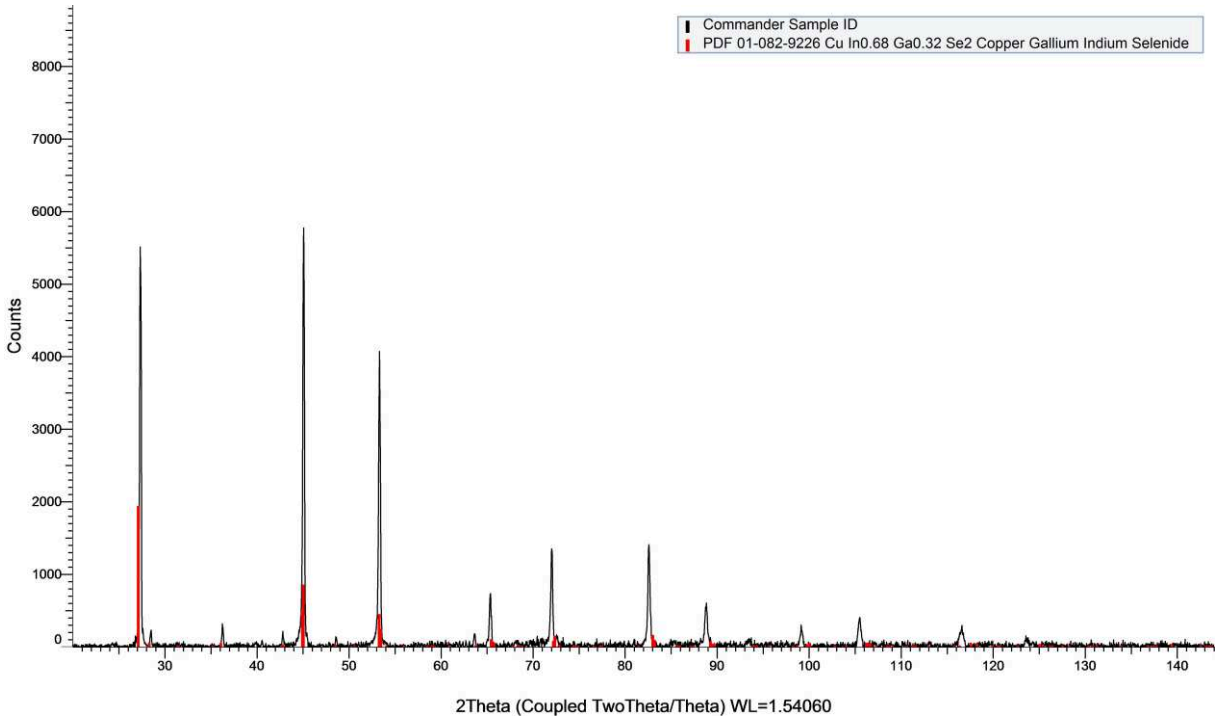

Figure 14. X-ray diffractogram of sample 5 after polishing away the graphite sheet from the pellet top and bottom.

The diffraction signal is much lower compared to the powder measurements due to the reduced measurement surface of the pellet. Otherwise all diffraction lines are

accounted for by the CIGS material and no new phases could be detected in the sintered pellet. The diffraction peaks do vary slightly in 2Θ angle but not more than it could be attributed to measurement uncertainty and non-perfect height leveling of the pellet during measurement. In total the material loss observed as pressure elevation during sintering did not however influence the composition of the final sintered material.

Economic impact on production costs

The cost of producing a sputtering target is in the end to be viewed as an underlying cost of production of the full solar cell modules. The economic impact on the production costs connected to manufacturing of the sputtering targets can further be divided into the cost of the CIGS material itself and the costs associated to the processing steps in the production. In the case of comparing spark plasma sintering to conventional pressure less sintering or hot pressing techniques it is the cost part associated to production that is affected and not the material cost part. About 30% of the production cost of the target is estimated to be associated to cost of the material, leaving 70% of the total cost belonging to the production steps [MID 18]. This is to be considered a rough estimate and not an absolute value but provides a basis from which further cost reduction estimations can be extrapolated. The 70% does not only include the sintering part but also steps like grinding of the final target and addition of the indium backing foil to the sputtering target. The sintering step is however more energy intensive compared to for example material grinding so treating the entire 70% as being sintering related costs is a somewhat skewed but workable first approximation. When sintering sputtering targets using for example hot pressing common dwell times of the isothermal pressing step used are on the order of about 2-3 hours long [LI 15, HSU 12, NIN 10]. Comparing the energy consumption by only comparing the isothermal dwell time during sintering becomes biased since the sintering time during SPS is so short that the heat ramp time actually is the dominating part of the sintering process. Instead of comparing against 3 minutes sintering time a more reasonable approach is to sum up the entire sintering time where current is applied during SPS (heating up and isothermal sintering times combined) which adds up to about 8-9 minutes of effective heating time. This comparison naturally assumes similar power output of the sintering equipment used which is a reasonable assumption during the isothermal sintering since the heat transfer from the sintering zone will be the cause of energy losses during sintering and heat insulation of the sintering system is an adjustable design parameter and not a unique feature of any of the different sintering techniques. The heating up step of the sintering process may vary in required power output since the different sintering techniques discussed normally don't work using equally fast heating ramps as one another. By excluding the heating ramp from hot pressing and pressure less sintering from the calculation it is however possible to obtain a conservative estimate of time and energy savings using SPS compared to the alternative techniques. Comparing 9 minutes sintering to 2 hours sintering shows that the energy savings using SPS end up on a level of 92.5%. So a rough estimation would

be that about 90% of the energy input during sintering could be saved using SPS compared to hot pressing. This would correspond to a reduction of 90% of the initial 70% that was process costs making it possible to cut 63% of the total production cost (material + process) of the sputtering target. It should however again be noted that this calculation is an estimation that does not include additional processing steps beyond sintering. The production of the sputtering target is estimated to be about 20% of the total production cost of the final solar cell module [MID 18] which could result in a total cost reduction of the solar cell module of about 12-13% using SPS for sintering sputtering targets compared to hot pressing.

Conclusions

In all cases examined it was possible to produce sintered CIGS pellets by SPS, however sintering at 400 °C resulted in a very porous material where very little sintering had occurred. When sintering in between 500-600 °C it was possible to produce high density compacts reaching up to 95-97% of theoretical density using a sintering time of only 3 minutes. Some material volatilization could be observed as system pressure increased slightly during sintering but no undesired phase formation could be observed in the sintered pellets. It was possible to re-deposit CIGS powder onto a polished sintered sample without any adhesion problems between the interphase of the substrate pellet and the deposited material. This is promising results for the possibility to re-sinter powder onto full size used CIGS sputtering targets. During electron microscopy imaging of the produced pellets it was difficult to assess any particle sizes or grain boundaries in the produced pellets. It did however look like some degree of partial melting occurred in the samples during sintering. When sintering new CIGS powder at 550 or 600 °C some melting of the powder during the sintering process was also visually confirmed by formation of solidified droplets on the end of the pressing die.

References

[HSU 12] Hsu, W.H., Hsiang, H.I., Yen, F.C., Shei, S.C., Yen, F.S., Low temperature sintered $CuIn_{0.7}Ga_{0.3}Se_2$ prepared by colloidal processing, 2012, Journal of the European Ceramic Society 32, pp. 3753-3757

[HSU 15] Hsu, W.H., Hsiang, H.I., Yen, F.C., Shei, S.C., Two-step sintering of nanocrystalline $Cu(In_{0.7}Ga_{0.3})Se_2$, 2015, Ceramics International 41, pp. 547-553

[LI 15] Li, X., Zhao, M., Zhuang, D., Cao, M., Ouyang, L., Guo, L., Sun, R, Fabrication of Se-rich $Cu(In_{1-x}Ga_x)Se_2$ quaternary ceramic target, 2015, Vacuum 119., pp. 15-18

[LI 15] Li, X., Zhao, M., Zhuang, D., Cao, M., Ouyang, L., Guo, L., Gao, Z., Sun, R, Influence of Na on sintering of $Cu(In,Ga)Se_2$ quaternary ceramic targets, 2015, Journal of Alloys and Compounds 636, pp. 335-340

[MID 18] Midsummer AB, Data estimated by Midsummer AB, E-mail correspondence

[NIN 10] Ning, Z., Da-Ming, Z., Gong, Z., An investigation on preparation of CIGS targets by sintering process, 2010, Materials Science and Engineering B 166, pp. 34-40

[ZHO 14] Zhou, J., Zhang, F., Xia, L., Synthesis of $CuIn_{0.7}Ga_{0.3}Se_2$ nanoparticles and its quaternary sputtering target, 2014, Applied Mechanics and Materials 483, pp. 65-70

Med stöd från:
VINNOVA
Energimyndigheten
FORMAS
STRATEGISKA INNOVATIONS-PROGRAM

Appendix

The administration supplement is submitted as a separate document together with this report.